IEEE Photonics Journal
An IEEE Photonics Society Publication

An Optical Pulse Shaping Scheme for Simultaneous Photonic Filtering and Digitizing Systems

Volume 12, Number 1, February 2020

Yiwei Sun
Guiling Wu
Sitong Wang
Wang Cheng
Jianping Chen

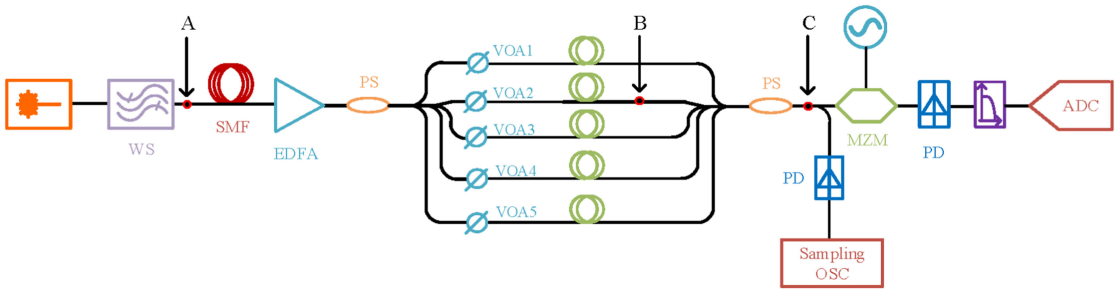

DOI: 10.1109/JPHOT.2020.2967809

An Optical Pulse Shaping Scheme for Simultaneous Photonic Filtering and Digitizing Systems

Yiwei Sun, Guiling Wu, Sitong Wang, Wang Cheng, and Jianping Chen

State Key Laboratory of Advanced Optical Communication Systems and Networks, Shanghai Institute for Advanced Communication and Data Science, Department of Electronic Engineering, Shanghai Jiao Tong University, Shanghai, Shanghai 200240, China

DOI:10.1109/JPHOT.2020.2967809

Manuscript received January 10, 2020; accepted January 14, 2020. Date of publication January 22, 2020; date of current version February 24, 2020. This work was supported by the National Natural Science Foundation of China under Grants 61535006, 61627817. Corresponding author: Guiling Wu (e-mail: wuguiling@sjtu.edu.cn).

Abstract: The equivalent filter response in the simultaneous photonic filtering and digitizing system is determined by the temporal precision and duration time of optical pulses. To achieve narrow-bandwidth filter response at high central frequency, a pulse shaping scheme based on the time-frequency mapping and attenuation-delay coupling is presented. The effect introduced by attenuation-delay coupling is derived, and the method to search optimized parameters for target bandwidth, off-band suppression and central frequency is presented. Precise shaping of optical pulses with full width at half-maximum in sub-nanosecond order is realized in experiments, which can generate an equivalent filter with bandwidth of 0.93 GHz and central frequency of 39.9 GHz in the simultaneous photonic filtering and digitizing system.

Index Terms: Pulse shaping, microwave photonics signal processing.

1. Introduction

Recently, an simultaneous photonic filtering and digitizing system [1]–[3] has been proposed. The system can achieve the integrated function of filtering and digitizing of input RF signals by combining optical pulse shaping and photonic analog-to-digital convertors (PADC), and therefore avoids multi-stage electro-optic and optic-electric conversion in the direct cascade of microwave photonic filters (MPFs) [4]–[6] and PADCs [7]–[9]. In simultaneous photonic filtering and digitizing systems, the received radio-frequency signals are filtered and modulated by a periodic optical pulse train, and then detected and digitized by low speed photodetector and ADC synchronized with the periodic optical pulse train. The output of the system is the sub-sampling of the received RF signals filtered by the equivalent filter. In the simultaneous photonic filtering and digitizing system, the equivalent filter impulse response is determined by the temporal shape of the optical sampling pulse and the impulse response accounting from the analog filter to the ADC [3]. Therefore, in the simultaneous photonic filtering and digitizing system, optical pulse shaping is one of the key issues, which is used to control the equivalent filter response. The central frequency and bandwidth of the equivalent filter response is mainly determined by the temporal precision and duration time of optical pulses. To achieve equivalent filter response with narrow bandwidth at high central

frequency, optical pulses with both high temporal precision and long duration time are required in simultaneous photonic filtering and digitizing systems. In previous work [1]–[3], since temporal precision and duration time of the generated optical pulses are limited by pulse shaping schemes, what can be achieved is equivalent filter response with either high central frequency and wide bandwidth of 10 GHz [1], or delicate bandwidth of 1 GHz and limited central frequency [2], [3]. This motivates us to explore other pulse shaping schemes suitable to be implemented in simultaneous photonic filtering and digitizing systems, so that the system can have narrow-bandwidth equivalent filter response at high central frequency.

Till to now, there are four typical optical arbitrary waveform generation (OAWG) schemes, namely, OAWG based on line-by-line Fourier transform [10], [11], OAWG based on direct time domain shaping [12], [13], OAWG based on temporal synthetization [14]–[16], and OAWG based on time-frequency mapping [17]–[19]. However, there are different limitations when each of the four types of schemes is applied in simultaneous photonic filtering and digitizing systems to realize high temporal precision optical pulse shaping with long duration time. OAWG based on line-by-line Fourier transform is limited on temporal shaping precision by the channel spacing of wavelength multiplexers when the optical pulse train with low repetition rate is used to release the bandwidth pressure on the back-end electrical process. For direct time domain shaping scheme, a pair of dispersion mediums with symmetric dispersion value is utilized to achieve pulse shaping by a modulator. The symmetric dispersive medium pair is difficult to manipulate, and the temporal precision of pulse shaping is degraded by the dispersive difference. In OAWG based on temporal synthetization, several copies of ultra-short optical pulses with different time delays and amplitudes are combined to generate optical pulses with designed temporal shapes. These schemes can generate optical pulses with high temporal precision. However, in order to generate longer pulses without degrading the temporal precision, the number of copies has to be greatly increased since the generated optical pulse is direct synthetized by ultra-short pulses [16]. The scheme based on time-frequency mapping maps the shaped spectrum profile to the time domain by the effect of dispersion. Without components with high spectrum shaping resolution, the scheme can reach high temporal shaping precision by dispersive modules with small dispersive value. However, small dispersive value will limit the reachable duration time of shaped optical pulses with certain optical spectrum width.

In this paper, an optical pulse shaping scheme is proposed to achieve narrow-bandwidth equivalent filter response at high central frequency in simultaneous photonic filtering and digitizing systems. The proposed scheme achieves the precise manipulation of optical pulses with full width at half-maximum (FWHM) in sub-nanosecond order by combining time-frequency mapping and attenuation-delay coupling. The attenuation-delay coupling is introduced to assist the time-frequency mapping scheme to remit the conflict between high temporal precision and long duration time. The attenuation and delay in the proposed scheme are determined by an optimization computation. The proposed scheme and theoretical analysis are verified by simulation and experiment in simultaneous photonic filtering and digitizing systems.

2. Modeling and Analysis

The schematic diagram of the proposed pulse shaping scheme based on time-frequency mapping and attenuation-delay coupling is shown in Fig. 1.

The optical pulse train generated by a mode-locked laser (MLL) is first spectrally shaped by a programmable optical filter (POF). Then it is sent to a dispersive medium to conduct the time-frequency mapping that generates a time-domain waveform similar to the shaped spectrum [18]. The shaped pulses train is distributed to multiple paths by a power splitter to introduce different delay and attenuation. Finally, the adjusted pulse trains are coupled together to generate the pulse train with the target temporal profile.

The optical field of the MLL with period of T_s can be simplified as a train of impulse function since the optical pulses are narrow enough compared with the impulse response of POF [20]. The optical

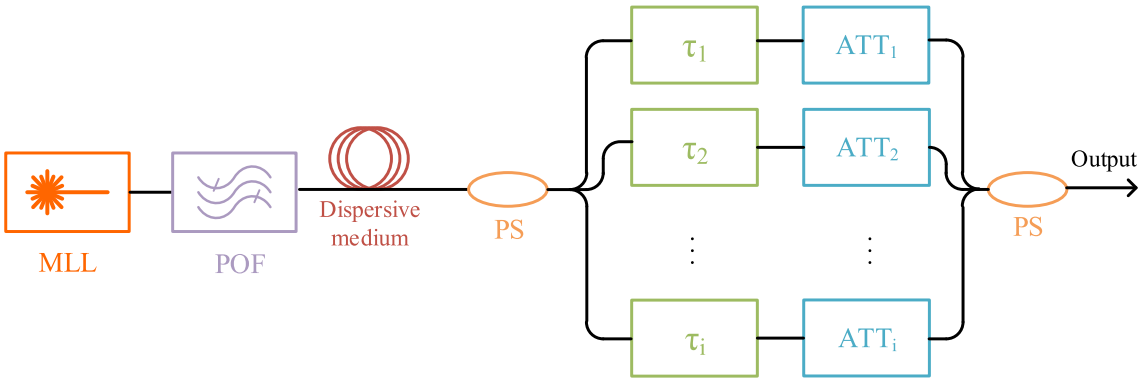

Fig. 1. Schematic diagram of optical pulse shaping based on time-frequency mapping and attenuation-delay coupling. MLL: mode-locked laser; POF: programmable optical filter; PS: power splitter; ATT: attenuator.

field after POF with the response of $h(t)$ can be expressed as

$$e_1(t) = \sum_{m=-\infty}^{\infty} \delta(t - mT_s) * h(t) = \sum_{m=-\infty}^{\infty} h(t - mT_s). \tag{1}$$

In Eq. (1), symbol * represents for convolution. The optical filed in frequency domain is

$$E_1(f) = \sum_{m=-\infty}^{\infty} \delta(f - m/T_s) \cdot H(f) = \sum_{m=-\infty}^{\infty} \delta(f - m/T_s) \cdot H(m/T_s), \tag{2}$$

where $H(f)$ is the amplitude-frequency response of POF. The spectrum of the pulse train after POF is a frequency comb with the same envelope as the filter response $H(f)$. When the dispersion value of the dispersive medium, $\ddot{\Phi}_\nu$ satisfies the far-field condition [21], the optical field after time-frequency mapping can be expressed as

$$\begin{aligned} e_2(t) &= e_1(t) * \exp\left(\frac{jt^2}{2\ddot{\Phi}_\nu}\right) = \exp\left(\frac{jt^2}{2\ddot{\Phi}_\nu}\right) \cdot \int_{\tau=-\infty}^{\infty} e_1(\tau) \cdot \exp\left(\frac{jt\tau}{\ddot{\Phi}_\nu}\right) d\tau \\ &= \exp\left(\frac{jt^2}{2\ddot{\Phi}_\nu}\right) \cdot \sum_{m=-\infty}^{\infty} \delta(f - m/T_s) \cdot H(m/T_s)|_{f=\frac{t}{\ddot{\Phi}_\nu}} \end{aligned} \tag{3}$$

Eq. (3) indicates that the shaped optical pulse is a scaled version of the programmable filter response $H(f)$ with a scale of $\ddot{\Phi}_\nu$. If there is only one path in the attenuation-delay coupling, for a fixed filter response $H(f)$, the dispersive value should be larger to form a shaped pulse with longer duration time while the temporal precision is degraded since the frequency resolution of POF is mapped to a larger time scale.

For attenuation-delay coupling scheme with multiple paths, suppose the amplitude-frequency response of POF is a multiplication of a Gaussian window and a cosine function, then the frequency response of POF can be shown as

$$H(f) = \exp\left(-\frac{(f - f_0)^2}{2\sigma_1}\right) \cdot [1 + \exp(2\pi f_{c,\lambda} \cdot j(f - f_0))], \tag{4}$$

where f_0 and σ_1 represent the mean and variance of the Gaussian window in optical domain while $f_{c,\lambda}$ is the frequency of the cosine function in amplitude-frequency response and the variance σ_1 indicates the optical spectrum range. It is to be noted that the response of POF is not limited to Gaussian shape, and therefore the generated optical shape will change to different shapes accordingly. To investigate the manipulation on the pulse shape, a single pulse is extracted from

the pulse train and investigated in the following part. The combined optical field of N paths, with attenuation and delay of $\{x_m, \tau_m\}$for mth path ($m = 1, 2, \ldots N$), can be derived as

$$e_{2,combined}(t) = \frac{1}{\sqrt{2}} \sum_{m=1}^{N} x_m \cdot \exp\left(-\frac{(t - t_0 - \tau_m)^2}{2\sigma_2}\right) \cdot [1 + \exp(2\pi j f_c(t - t_0 - \tau_m))], \tag{5}$$

where $t_0 = \ddot{\Phi}_\nu \cdot f_0$, and $\sigma_2 = \ddot{\Phi}_\nu^2 \cdot \sigma_1$ represent the mean and variance of the Gaussian window respectively. $f_c = f_{c,\lambda}/\ddot{\Phi}_\nu$ is the frequency of the cosine function after time-frequency mapping. The intensity of the combined pulses in time domain is the multiplication of the optical field in Eq. (5) and its complex conjugate $e^*_{2,combined}$. It can be derived as

$$\begin{aligned}
I(t) &= e_{2,combined} \cdot e^*_{2,combined}(t) \\
&= \frac{1}{2}\left\{\sum_{m=1}^{N} x_m \cdot \exp\left(-\frac{(t - t_0 - \tau_m)^2}{2\sigma_2}\right) \cdot [1 + \exp(2\pi j f_c (t - t_0 - \tau_m))]\right\} \\
&\quad \cdot \left\{\sum_{m=1}^{N} x_m \cdot \exp\left(-\frac{(t - t_0 - \tau_m)^2}{2\sigma_2}\right) \cdot [1 + \exp(2\pi j f_c (t - t_0 - \tau_m))]\right\}^* \\
&= \frac{1}{2}\left\{\sum_{m=1}^{N} 2x_m^2 \cdot \exp\left(-\frac{(t - t_0 - \tau_m)^2}{\sigma_2}\right) \cdot \left[2 + e^{2\pi j f_c(t - t_0 - \tau_m)} + e^{-2\pi j f_c(t - t_0 - \tau_m)}\right]\right. \\
&\quad + \sum_{m=1}^{N} \sum_{n=1, n\neq m}^{N} x_m x_n \cdot \exp\left(-\frac{(t - t_0 - \tau_m)^2}{2\sigma_2}\right) \cdot \exp\left(-\frac{(t - t_0 - \tau_n)^2}{2\sigma_2}\right) \\
&\quad \left. \cdot \left[1 + e^{2\pi j f_c(t - t_0 - \tau_m)} + e^{-2\pi f_c(t - t_0 - \tau_n)} + e^{2\pi j f_c(\tau_n - \tau_m)}\right]\right\}
\end{aligned} \tag{6}$$

By Fourier transform, the intensity of the combined pulses in frequency domain, or intensity spectrum, is derived as

$$\begin{aligned}
I_{combined}(f) = &\left\{\sum_{\substack{m=1 \\ >m}}^{N} x_m \cdot x_n \cdot \left[\exp(-j2\pi f_c(t_0 + \tau_m)) + \exp(-j2\pi f_c(t_0 + \tau_n))\right]\right. \\
&\cdot \exp\left(-\frac{(\tau_m - \tau_n)^2}{4\sigma_2}\right) \cdot \exp\left(-j2\pi(f - f_c)\left(t_0 + \frac{1}{2}(\tau_m + \tau_n)\right)\right) \\
&\left. + \sum_{m=1}^{N} {x_m}^2 \cdot \exp(-j2\pi f(t_0 + \tau_m))\right\} \\
&\cdot \sqrt{\sigma_2 \pi} \cdot \pi \cdot \exp\left(-\left(\pi\sqrt{\sigma_2}(f - f_c)\right)^2\right).
\end{aligned} \tag{7}$$

For simultaneous photonic filtering and digitizing systems, the intensity spectrum of the combined pulses corresponds to the passband of the equivalent filter response [3] [22]. In Eq. (7), the last Gaussian item is the passband for optical pulses before attenuation-delay coupling. After attenuation-delay coupling, the passband is modified by the real part of the item in the brace, which is determined by the delay and attenuation of each path. Eq. (7) indicates that both central frequency and bandwidth of the equivalent filter response can be reconfigured as designed by configuring proper delay and attenuation and reconfiguring the frequency response of POF.

TABLE 1
Optimized Parameters for the Passband of 1 GHz at 40 GHz

	Path 1	Path 2	Path 3	Path 4	Path 5
Attenuation(dB)	−3.1	−0.5	0	−0.7	−3.0
Delay(ns)	0	0.227	0.428	0.678	0.933

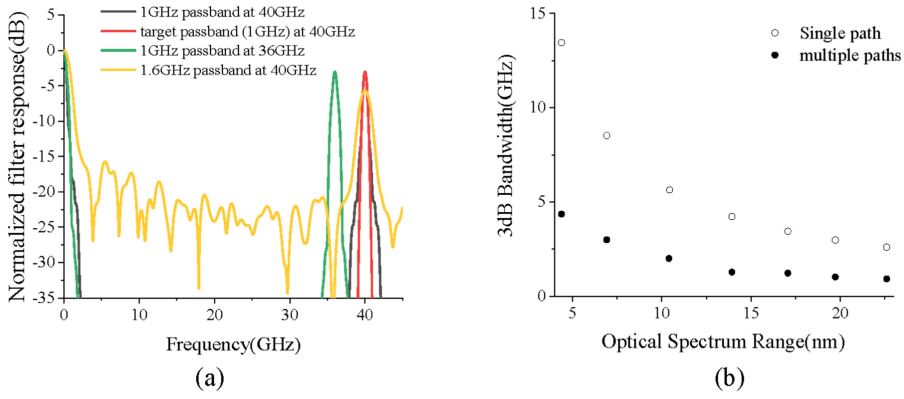

Fig. 2. (a) The target passband and passbands with optimized parameters. (b) The minimum 3 dB bandwidth for passband formed by single path and 5 paths via the optical spectrum range.

The delay and attenuation parameters for a target passband can be found by solving the optimization problem

$$\min\left[k_1 \cdot abs\left(\frac{f_{c\_ideal}}{f_c}-1\right)+k_2 \cdot abs\left(\frac{pb_{ideal}}{pb}-1\right)+k_2 \cdot abs\left(\frac{sp_{ideal}}{sp}-1\right)\right] \quad (8)$$
$$\text{s.t. } f_{c\_ideal}\cdot\tau_i \in \text{int},$$

where f_{c_ideal} is the target passband central frequency, pb_ideal is the target 3 dB bandwidth, and sp_ideal is the target off-band suppression. k_i represents the weights, which can be adjusted to emphasize certain characteristic of the passband according to practical application requirements. The constraint ensures the real part of the item in brace in Eq. (8) to reach its maximum at the frequency of f_{c_ideal}.

Table 1 shows a set of optimized parameters for a target passband with central frequency of 40 GHz, 3 dB bandwidth of 1 GHz (corresponding the FWHM of 0.7 ns), and the off-band suppression of more than 20 dB when the optical spectrum range of the incident optical pulses and dispersive value are 12 nm and 100 ps/nm respectively. The passband formed according to parameters in Table 1 is depicted in Fig. (2)(a) in black together with the target passband in red. The passband utilizing the optimized parameters in Table 1 has the same central frequency and 3 dB bandwidth as the target passband, and its passband profile agrees well with the target passband. Other optimized passbands with central frequency at 31 GHz and 36 GHz, together with an optimized passband with central frequency of 40 GHz and bandwidth of 1.6 GHz are depicted in Fig. (2)(a) to illustrate the validity of the optimization problem in finding the parameters according to practical application requirements.

Fig. (2)(b) shows the simulated minimum 3 dB bandwidth of a passband formed in a 5-path attenuation-delay coupling scheme under different optical spectrum ranges. The passband has the central frequency of 40 GHz and off-band suppression >20 dB, and the spectrum resolution of POF is set to 0.08 nm and $\ddot{\Phi}_v = 100$ ps/nm in the simulation. For comparison, the bandwidth of passbands formed by single path in the same conditions are also shown in Fig. (2)(b). It indicates that the proposed attenuation-delay coupling scheme can obtain a passband with a

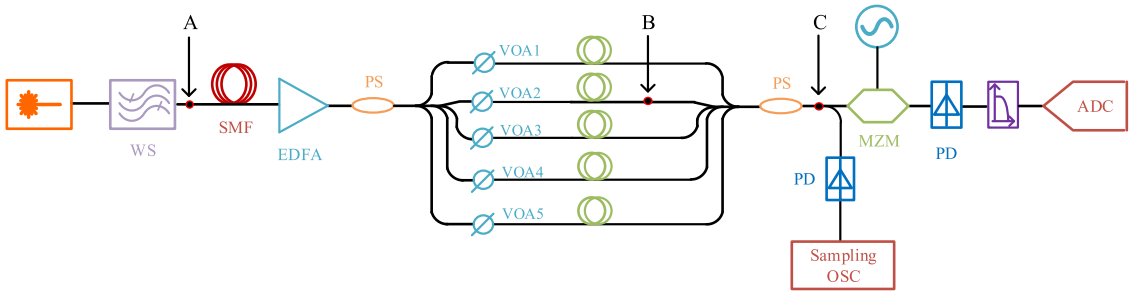

Fig. 3. Experiment setup for verification of optical pulse shaping scheme based on time-frequency mapping and delay-attenuation coupling. MLL: mode-locked laser; WS: Waveshaper; SMF: single mode fiber; EDFA: Erbium-doped fiber amplifier; VOA: variable optical attenuator; PS: power splitter; MZM: Mach-Zehnder modulator; PD: photodiode; Sampling OSC: sampling oscilloscope.

narrower available minimum 3 dB bandwidth while adopting the same optical spectrum range. As a result, the proposed scheme achieves high temporal shaping precision and long duration time simultaneously without increasing the optical spectrum range. By means of attenuation-delay coupling, without increasing the optical spectrum range, it remits the conflict between high temporal shaping precision and long duration time in OAWG scheme based on time-frequency mapping.

3. Experimental Verification

In order to verify the proposed pulse shaping scheme based on time-frequency mapping and attenuation-delay coupling, an experiment based on simultaneous photonic filtering and digitizing systems utilizing the given scheme has been carried out. The experiment setup is shown in Fig. 3. In the experiment, a Finisar Waveshaper 16000 s was used as POF with the setting resolution of 0.08 nm to shape the incident optical pulse train generated by a mode-locked laser with 36.5 MHz repetition rate and 14 nm linewidth. A 6.5 km *G*652.*d* single mode fiber (SMF) was used as the dispersive medium of $\sim$100 ps/nm. After pulse shaping, the incident optical pulses were amplified by an erbium-doped fiber amplifier (EDFA) and divided into five paths with variable optical attenuators (VOAs) and delay lines to control the attenuation and delay respectively. Since the whole experiment was conducted in an air-conditioned room, and the total lengths of fibers in different paths are small, no extra control on phase stability was implemented during the experiment. After introducing attenuation and delays as designed, the pulses in multiple paths were coupled together and sent to a 40 GHz Mach-Zehnder modulator biased at quadrature point to be modulated by the RF signal generated by a microwave signal generator. The microwave signal generator was controlled by the digitizer. The modulated pulse train was detected and digitized by a photodiode with 100 MHz bandwidth and a digitizer with an analog bandwidth of 650 MHz. By digitizing the input analog signal at various frequency points, the equivalent filter response was measured. For the measurement on the temporal intensity of the shaped optical pulses, a 50 GHz PD and a 70 GHz sampling oscilloscope (Keysight, DCA-X 86100D with 86118 A module) were utilized.

The optical spectrum of the pulses after Waveshaper, which was measured at point A in Fig. 3, is shown in Fig. 4(a). The spectrum shaping resolution of the POF was 0.08 nm, and the optical spectrum range was 12 nm. Fig. 4(b) shows the measured pulse waveform at B and C respectively. For pulses measured at point C, the delay and attenuation were set according to the optimized parameters in Table 1. Pulses formed by multiple paths indicate that the scheme based on attenuation-delay coupling can generate shaped optical pulses with the FWHM of 0.7 ns. Next, the intensity spectra were calculated by Fourier transform from the temporal pulse's waveform in Fig. 4(b) and are shown in Fig. 4(c). The intensity spectra can simulate the equivalent filter response of the optical pulses shaped by single path and multiple paths [1]. The simulated equivalent filter

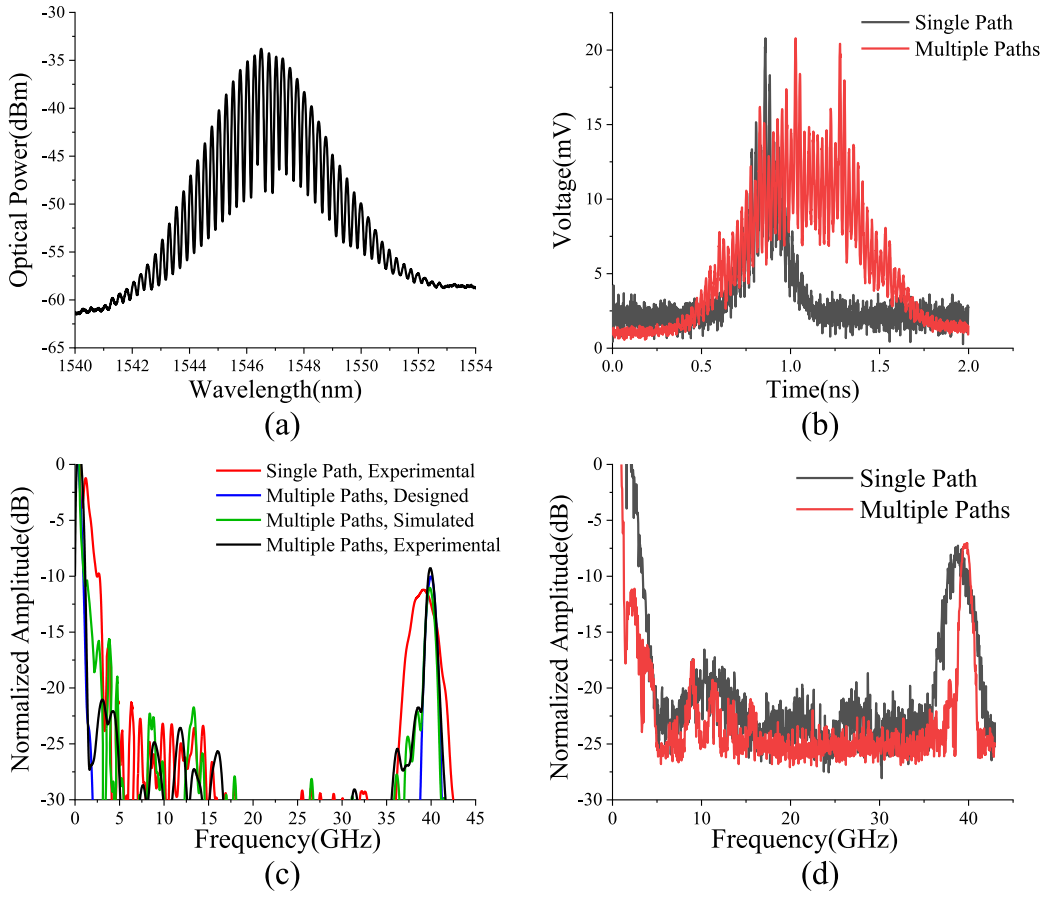

Fig. 4. (a) Optical spectrum after filtered by Waveshaper, (b) Shaped optical pulse without and with multiple paths' delay-attenuation coupling, (c) Intensity spectrum of the pulses in simulation and experiment, (d) the frequency response of the simultaneous photonic filtering and digitizing system with pulses shaped by single path and multiple paths of delay-attenuation and coupling.

responses indicate that the 3 dB bandwidth is reduced from 2.44 GHz to 0.99 GHz when multiple paths were coupled together. Then, the intensity spectrum of optical pulses formed by the optimized parameters in Table 1 was simulated based on an available optical spectrum range of 12 nm and a 100 ps/nm dispersive medium. It is depicted as the designed filter response in Fig. 4(c). The filter response simulated through experiment result is similar to the designed filter response in bandwidth and central frequency, however, it has some disagreement on the passband profile. This is mainly due to the distortion in time-frequency mapping and the setting error of the parameters in the experiment. At last, another simulation concerning the possible causes was conducted and its result is depicted in Fig. 4(c) as the simulated filter response, which fits well with the intensity spectrum of optical pulses shaped by multiple paths in experiment. Therefore, it proves that the parameters setting error and waveform distortion during the time-frequency-mapping are two major causes in passband distortion.

The equivalent filter responses of the pulse trains shaped by single path and multiple paths were measured and the measurements are depicted in Fig. 4(d). The measured equivalent filter responses in Fig. 4(d) indicate that equivalent bandpass filters with central frequency at 38.74 GHz and 39.9 GHz are formed. The 3 dB bandwidth is decreased from 2.34 GHz to 0.93 GHz as multiple paths were coupled together to form the generated pulses. The difference on the bandwidth between the measured and simulated equivalent filter response is due to the slight change on the optical pulses during the experiment. The measured equivalent filter response in Fig. 4(d)

agrees well with the simulated filter response based on measured optical pulses. Consequently, the experiment results verify that the simultaneous photonic filtering and digitizing systems utilizing this scheme can achieve an equivalent filter working at 39 GHz with the bandwidth of 0.93 GHz with limited spectrum range of 12 nm. Unlike the time-frequency mapping scheme which either degrades central frequency or increases optical spectrum range, the proposed scheme can narrow bandwidth without the degradation or increase.

4. Conclusion

An optical pulse shaping scheme based on time-frequency mapping and attenuation-delay coupling is presented in this paper. Optical pulses without large optical spectrum range can be shaped into long pulses with high temporal precision to realize the simultaneous photonic filtering and digitizing systems with narrow-bandwidth equivalent filter responses at high central frequency. The effect introduced by attenuation-delay coupling are derived, and the method to search optimized parameters for target bandwidth, off-band suppression and central frequency is presented. A proposed scheme with a dispersive medium of 100 ps/nm and 5-path attenuation-delay coupling is simulated and experimentally verified. A 0.7 ns (FWHM) pulse with temporal precision of 0.025 ns is obtained by shaping an incident 12 nm pulse, which can achieve an equivalent filter response with a Gaussian-like passband of 0.93 GHz at central frequency of 39.9 GHz in simultaneous photonic filtering and digitizing systems. The proposed scheme can also generate pulses in other shapes than the Gaussian-like one by changing the response of the POF, and therefore it can form equivalent filter responses with different passband shapes and adjustable central frequency.

References

[1] F. Su, G. Wu, and J. Chen, "Photonic analog-to-digital conversion with equivalent analog prefiltering by shaping sampling pulses," *Opt. Lett.*, vol. 41, no. 12, pp. 2779–2782, 2016.
[2] S. Wang, G. Wu, F. Su, and J. Chen, "Simultaneous microwave photonic analog-to-digital conversion and digital filtering," *IEEE Photon. Technol. Lett.*, vol. 30, no. 4, pp. 343–346, Feb. 15, 2018.
[3] S. Wang, G. Wu, Y. Sun, and J. Chen, "Principle of integrated filtering and digitizing based on periodic signal multiplying," *Opt. Lett.*, vol. 44, no. 7, pp. 1766–1769, 2019.
[4] P. Li, W. Pan, X. Zou, B. Lu, and L. Yan, "Fast tunable photonic single-bandpass RF filter with multiple arbitrary switching flat-top passbands," *J. Lightw. Technol.*, vol. 36, no. 19, pp. 4583–4590, 2018.
[5] J. Capmany, B. Ortega, and D. Pastor, "A tutorial on microwave photonic filters," *J. Lightw. Technol.*, vol. 24, no. 1, pp. 201–229, 2006.
[6] Z. Zeng *et al.*, "Freely tunable dual-passband microwave photonic filter based on phase-to-intensity modulation conversion by stimulated brillouin scattering," *IEEE Photon. J.*, vol. 11, no. 1, pp. 1–9, 2019.
[7] C. Xu, S. Zheng, X. Chen, H. Chi, X. Jin, and X. Zhang, "Photonic-assisted time-interleaved ADC based on optical delay line," *J. Opt.*, vol. 18, no. 1, p. 015704, 2015.
[8] G. C. Valley, "Photonic analog-to-digital converters," *Opt. Express*, vol. 15, no. 5, pp. 1955–1982, 2007.
[9] H. He *et al.*, "An improved photonic analog-to-digital conversion scheme using Mach–Zehnder modulators with identical half-wave voltages," *Opt. Commun.*, vol. 425, pp. 157–160, 2018.
[10] R. Proietti *et al.*, "Elastic optical networking by dynamic optical arbitrary waveform generation and measurement," *J. Opt. Commun. Netw.*, vol. 8, no. 7, pp. A171–A179, 2016.
[11] S. Feng *et al.*, "Rapidly reconfigurable high-fidelity optical arbitrary waveform generation in heterogeneous photonic integrated circuits," *Opt. Express*, vol. 25, no. 8, pp. 8872–8885, 2017.
[12] S. Thomas, A. Malacarne, F. Fresi, L. Potì, and J. Azaña, "Fiber-based programmable picosecond optical pulse shaper," *J. Lightw. Technol.*, vol. 28, no. 12, pp. 1832–1843, 2010.
[13] J. Huh and J. Azaña, "In-fiber reconfigurable generation of arbitrary (asymmetric) picosecond temporal intensity waveforms by time-domain optical pulse shaping," *Opt. Lett.*, vol. 41, no. 4, pp. 693–696, 2016.
[14] R. Ashrafi, J. Azaña, and L. R. Chen, "Tunable optical arbitrary waveform generation based on time-delay to intensity mapping," in *Proc. IEEE Photon. Conf.*, 2014, pp. 308–309.
[15] S. Liao *et al.*, "Arbitrary waveform generator and differentiator employing an integrated optical pulse shaper," *Opt. Express*, vol. 23, no. 9, pp. 12161–12173, 2015.
[16] M. Shen and R. A. Minasian, "Toward a high-speed arbitrary waveform generation by a novel photonic processing structure," *IEEE Photon. Technol. Lett.*, vol. 16, no. 4, pp. 1155–1157, Apr. 2004.
[17] J. Chou, Y. Han, and B. Jalali, "Adaptive RF-photonic arbitrary waveform generator," *IEEE Photon. Technol. Lett.*, vol. 15, no. 4, pp. 581–583, Apr. 2003.
[18] J. Azana, "Design specifications of time-domain spectral shaping optical system based on dispersion and temporal modulation," *Electron. Lett.*, vol. 39, no. 21, pp. 1530–1532, 2003.

[19] H. Chi and J. Yao, "Fiber chromatic dispersion measurement based on wavelength-to-time mapping using a femtosecond pulse laser and an optical comb filter," *Opt. Commun.*, vol. 280, no. 2, pp. 337–342, 2007.
[20] Z. Jin, G. Wu, C. Wang, and J. Chen, "Mismatches analysis based on channel response and an amplitude correction method for time interleaved photonic analog-to-digital converters," *Opt. Express*, vol. 26, no. 14, pp. 17859–17871, 2018.
[21] D. E. Leaird *et al.*, "Dispersion requirements in coherent frequency-to-time mapping," *Opt. Express*, vol. 19, no. 24, pp. 24718–24729, 2011.
[22] F. Su, G. Wu, L. Ye, R. Liu, X. Xue, and J. Chen, "Effects of the photonic sampling pulse width and the photodetection bandwidth on the channel response of photonic ADCS," *Opt. Express*, vol. 24, no. 2, pp. 924–934, 2016.